RSC Advances

PAPER

View Article Online
View Journal | View Issue

Cite this: *RSC Adv.*, 2025, **15**, 12162

Water-borne chitosan/CuO-GO nanocomposite as an antibacterial coating for functional leather with enhanced mechanical and thermal properties†

Khandaker Tanzim Rahman,[ab] Md. Nur-E. Alam[c] and M. Nuruzzaman Khan *[a]

The advancement of eco-friendly and effective antibacterial outer surfaces for medical textiles and leather products is considered important by industries and end users. Herein, positively charged chitosan (CS) and copper oxide nanoparticle-decorated negatively charged graphene oxide (CuO-GO) were assembled layer-by-layer to create an innovative nanocomposite (CS/CuO-GO) coating onto the leather surface. GO was prepared from graphite powder. Eco-friendly synthesis of CuO nanoparticles with *Aloe vera* leaf extract was reported and utilized to prepare the CuO-GO nanocomposite. The as-prepared materials were tested through FTIR, XRD, UV-vis spectroscopy, TEM, and DLS analyses. Different amounts of CS/CuO-GO coated leathers showed efficient antibacterial activities against *Escherichia coli* (*E. coli*) and *Bacillus subtilis* (*B. subtilis*) using a "kill-release" approach. This was largely attributed to the cooperative interaction between the contact-killing of the chitosan layer, the discharge of Cu^{2+} ions, and the bacterial-repelling properties of the anionic GO layer. The FE-SEM analysis confirms the existence of a CuO-GO layer on the leather surface with an effect on the macroscopic level performances. The XPS analysis confirms the chemical state of the coated materials on the leather surface. Tensile, tear, and stitch tear strength increased after coating with the CS/CuO-GO nanocomposite. The WVP of the coated leather remains within the range after coating with different wt% of the CS/CuO-GO nanocomposite. The durability of the nanocomposite coating on leather surfaces was thoroughly examined through dry and wet rub fastness tests. Results clearly showed that the strong coating greatly enhanced the antibacterial effectiveness of leather against mechanical wear. The impacts of CS/CuO-GO nanocomposite coating on the leather surface hydrophilicity were evaluated using water contact angle measurements. Water-borne chitosan-based CuO-GO nanocomposite showed a good eco-friendly leather finishing system. It could extend their applications to sports and medical textiles to impart antibacterial effects.

Received 9th January 2025
Accepted 2nd April 2025

DOI: 10.1039/d5ra00225g

rsc.li/rsc-advances

1 Introduction

In recent decades, research on nanomaterials has received substantial consideration from academics and industrial researchers owing to their unique catalytic, thermoelectric, mechanical, and optical properties. An outstanding feature of nanoparticles is their effective antibacterial activity. There has been a growing interest in bactericidal coatings designed to eliminate adherent bacteria. For instance, the utilization of nanoparticle-based antibacterial coatings on functional surfaces is gaining popularity owing to their myriad of benefits and versatile advantages.[1] A wide range of nanomaterials are reported to be microbiocidal and used for the fabrication of functional surface coating, which include MOFs,[2,3] PAN-nanopolymers,[4] silver and palladium salt precursors,[2,5–7] and carbon quantum dots.[8] The surface coating of various functional materials with nanoparticles to impart desired properties is an attractive approach for biocidal coatings. A variety of metal and metal oxide nanoparticles (NPs), including Ag NPs, TiO_2 NPs, CuO NPs, ZnO NPs, Se NPs, and their nanocomposites, are employed to make antimicrobial-coated surfaces.[9,10] Unfortunately, numerous materials and methods have been employed to produce antibacterial products that are not eco-friendly, hazardous to people, and promote the growth of antibiotic-resistant germs.

[a]*Department of Applied Chemistry and Chemical Engineering, Faculty of Engineering and Technology, University of Dhaka, Dhaka, 1000, Bangladesh. E-mail: mnuruzzaman.khan@du.ac.bd*

[b]*Institute of Leather Engineering and Technology, University of Dhaka, Dhaka, 1000, Bangladesh*

[c]*Leather Research Institute, Bangladesh Council of Scientific and Industrial Research, Dhaka, Bangladesh*

† Electronic supplementary information (ESI) available: XRD of CuO NPs, the zeta potential of CuO-GO nanocomposite, the particle size analysis of CuO NPs, the optical images of leather before and after coating, the weight loss curve of chitosan, CuO-NPs, GO, and CuO-GO, an antibacterial test of CS/CuO-GO nanocomposite coated leather at bacterial concentration of 108 CFU mL^{-1}. See DOI: https://doi.org/10.1039/d5ra00225g

Graphene oxide (GO) is a 2D carbon material with a high surface area to volume ratio and exceptional antibacterial, electrical, thermal, mechanical, and optical properties. It exhibits excellent antibacterial properties primarily attributed to its numerous physical or chemical interactions with bacterial cells, thus eliciting a potent antibacterial effect. The cutting edges of GO nanosheets harm the cell membrane during physical contact.[11] It contains hydroxyl, epoxy, carboxyl, and carbonyl functional groups on the basal planes, which are usually formed by the chemical oxidation of graphite.[12] These functional groups effectively react with polymers to yield hybrid materials. The incorporation of GO with varying flake sizes into different polymer matrices to achieve specific properties has been reported elsewhere.[13] However, the aggregation of GO nanosheets due to the van der Waals forces could result in poor enhancement of the physical properties of the nanocomposites. Recent techniques have demonstrated effectiveness in minimizing the agglomeration of graphene oxide within polymer matrices. For instance, Kale *et al.* synthesized GO-silica nanocomposite as nanofillers in the waterborne polyurethane (WPA) matrix and coated them on leather surfaces.[14] A significant improvement was observed in the tear resistance, surface adhesion, and abrasion resistance properties due to the reduced clusters of GO in WPA. Similar results were reported for nanocomposites comprising graphene oxide and metal oxides, *viz.* ZnO, TiO_2, Ag, CuO *etc.*[11,15,16] Similarly, Cu and its oxide-based composites are very popular for their eco-richness, effortless preparation, and coating of clinical equipment due to their biocidal effects. CuO NPs appear to have varied antibacterial action depending on the characteristics of the bacterial cells. For instance, the gram nature of their cellular walls appears to influence the antibacterial action of CuO NPs. When CuO NP concentrations greater than 9.5% were applied, 100% of Gram-negative *Escherichia coli* cells were destroyed; however, there was a reduced killing efficiency against Gram-positive *Staphylococcus aureus*.[17]

Therefore, GO could be a suitable platform to host and be functionalized with CuO. This hybridization of GO and CuO is known to improve the active sites, include superior functionality and significantly reduce the agglomeration of GO nanosheets. These CuO-GO nanocomposites can be synthesized by a facile bottom-up technique, without loss of their potential for antibacterial and antioxidant activities.[18]

Leather is a breathable, soft, flexible, long-lasting, and comfortable material that has been chosen as a suitable material for biocidal coating. Several approaches have been undertaken to create different antibacterial coating materials that can effectively decrease bacterial adhesion and prevent biofilm development.[19] Natural polycationic materials like biocompatible chitosan (CS), known for their contact-active distraction of the microbe cytoplasmic layer, have been widely employed in the advancement of bactericidal coatings.[20] The antibacterial properties of cationic polymers may be reduced when they are immobilized on a substrate, limiting their diffusion into cell membranes.[21] Besides, the chitosan films possess lower mechanical properties, air–vapour permeability, and hydrophilicity.

To address this limitation, several nanofiller materials with distinct properties can be used to enhance the mechanical strength and water permeability. For example, Liu *et al.* synthesized a nanoparticle coating composed of PEGylated CS-protected Ag NPs (PEG-g-CS/AgNPs), and the surface properties were enhanced after the application of such composite.[22] In addition, the slow release of biocidal Ag^+ ions gradually eliminates bacteria in the environment. This potent efficacy stems from the dual mechanisms of bacteria shielding and discharge through PEGylation, along with the double bacteria-killing properties derived from CS and the discharge of Ag^+ ions.

Inspired by these interesting research outcomes, copper oxide nanoparticles decorated negatively charged graphene oxide (CuO-GO) and positively charged chitosan (CS) were assembled layer-by-layer (LBL) to form a nanocomposite (CS/CuO-GO) coating on the leather surface. The CuO nanoparticles were synthesized using *Aloe vera* plant extract. The functionalization of CuO nanoparticles on GO flakes may prevent the agglomeration of GO and enhance the uniform coating of GO onto the leather surface. Moreover, the combined antibacterial and antifungal properties of CuO-GO were improved to some extent. Additionally, chitosan and the CuO-GO nanocomposite were applied using LBL spray-coating with PVA as an adhesive on the leather surface. The influence of the CS/CuO-GO coating on the morphological-, thermal-, mechanical-, and cyclic antibacterial effects was investigated. The novel CS/CuO-GO coated leather was evaluated for abrasion and tear resistance, and water vapor permeability. To the best of our knowledge, this is the first study of LBL spray-coating of CS/CuO-GO nanocomposite on leather surface and it may lead to an innovative approach to using nanomaterial as surface coating in industry with extensively improved biocompatible polymer composite.

2 Materials and methods

2.1 Materials

Crust bovine leather was supplied by Reliance Tannery Ltd (Hemayetpur-Savar, Dhaka, Bangladesh). *Bacillus subtilis* and *E. coli* were donated by the microbiology lab at the University of Dhaka. Polyvinyl alcohol (PVA) (MW = 115 000 g mol^{-1}), potassium permanganate ($KMnO_4$), nutrient agar, and nutrient broth were procured from Research lab Fine Chem, India. Chitosan flakes (degree of diacylation, 90%; viscosity, 10–150 mPa s) were purchased from Sisco, India. Sodium hydroxide (NaOH), 37 wt% hydrochloric acid (HCl), and glacial acetic acid (CH_3COOH) were bought from Merck, India. Sodium nitrate ($NaNO_3$) and copper nitrate trihydrate ($Cu(NO_3)_2 \cdot 3H_2O$) were sourced from Loba Chemic, India, and Sigma Aldrich, Germany provided conc. sulfuric acid (H_2SO_4), conc. nitric acid (HNO_3), and 30 wt% hydrogen peroxide (H_2O_2). Graphite powder (C) was sourced from Uni-Chem, China.

2.2 Preparation of graphene oxide (GO)

The synthesis of GO was conducted by adapting the modified Hummer's method.[23] Initially, a 3 : 1 (w/v) mixture of H_2SO_4 (57

mL) and HNO_3 (18 mL) was prepared. Then, graphite powder (3.0 g) was dispersed in the mixture with vigorous stirring for 15 min at room temperature. Subsequently, $KMNO_4$ (9.0 g) and $NaNO_3$ (1.5 g) were added in small portions over 30 min. After that, the mixture was stirred for 2 h at 25 °C, and then magnetically stirred for 12 h at room temperature to form a paste. Distilled water (90 mL) was added to the paste and stirred for 3 h at 35 °C to produce a deep brown mixture. 300 mL of distilled water and 30% H_2O_2 were added continuously into a deep brown mixture until it turned yellow. Finally, the mixture was treated with 5% HCl (200 mL) to remove manganese ions, washed to reach a neutral pH, and then dried at 60 °C.

2.3 Green synthesis of CuO nanoparticles

The eco-friendly synthesis of CuO NPs was achieved using *Aloe vera* (*Aloe barbadensis* Miller) extract following an environmentally benign method.[24] Initially, *Aloe vera* leaves were washed thoroughly, sliced, dried, and then boiled in 250 mL of water in a flask at 100 °C for 15–20 min. The extract was cooled, filtered in two steps, and kept at 4 °C. In the next phase, 5 mL of the *Aloe vera* extract and 50 mL of 0.01 mol L^{-1} of copper nitrate solution were combined and vigorously stirred at 100–120 °C for 24 h. The solution showed a color transformation from deep blue to light green, and finally to brownish red, signalling the formation of CuO NPs. Subsequently, the solution was centrifuged at 8000 rpm for 20 min. The precipitate was dried in an oven dryer at 105 °C for 20 h. Finally, the dark brown CuO NPs were calcined in a muffle furnace at 500 °C for 6 h before further use.

2.4 Preparation of CuO-GO nanocomposites (CuO-GO NCs)

CuO-GO nanocomposite was prepared following the reported method[25] with modifications. Initially, 1 g GO was suspended in 200 mL of distilled water and ultrasonicated for 2 h at ambient temperature. Concurrently, 0.4 g of CuO NPs were dissolved in 100 mL of distilled water. These two solutions were then mixed and ultrasonicated for 1 h at RT. The combination was then heated to 85 °C for 2.5 h and allowed to cool. Following this, the mixture was centrifuged at 8000 rpm for 20 min, washed with distilled water and ethanol until a neutral pH was achieved, and dried in an oven at 60 °C for 8 h.

2.5 LBL coating of chitosan and CuO-GO onto leather

At first, 2 wt% of chitosan solution was mixed with PVA (5 wt% of chitosan) solution for proper binding with the leather surface. Then, 1 mg mL^{-1} and 5 mg mL^{-1} of CuO-GO were separately dispersed in water by sonication for 3 h. Chitosan solution was sprayed onto the leather surface, properly dried, and the aqueous dispersion of CuO-GO nanocomposite was spray-coated onto the chitosan-coated leather surface. Finally, CuO-GO-embedded chitosan-coated leather was obtained after proper drying. This process was carried out two times to impart double coating on the leather surface. Pristine leather, chitosan-coated leather, and 1 mg mL^{-1} and 5 mg mL^{-1} of CS/CuO-GO NCs coated leather were prepared (Scheme 1) for analysis.

2.6 Characterization techniques

The surface morphology of the as-prepared nanocomposite coated surface was analysed on an ultra-high-resolution FE-SEM (JSM-7610F, Jeol, Japan) at acceleration voltages ranging from 0.1 kV to 30 kV. With an accelerating voltage of 5–10 kV, a secondary electron detector was used to observe the surfaces of the specimen. XPS survey spectra and HR-XPS scan spectra were attained using an Escalab Xi+ system (Thermo Fisher Scientific, Czech Republic). The survey scans were obtained using an Al Kα gun having a spot size of 500 μm, a step size of 1.00 eV, a pass energy of 50.0 eV, and 10 scans for thorough analysis. In the HR-XPS spectra analysis, the pass energy was 10.0 eV, and the step size was 0.10 eV. A total of 10 scans were conducted for the C 1s and O 1s measurements, while 30 scans were performed for N 1s. Fourier transform infrared spectra were measured with an FTIR instrument (Bruker, Alpha II, Germany) over the range of 400 cm^{-1} to 4000 cm^{-1} with a scan number of 128. X-ray Diffraction was analysed on a Bruker AXS D8 diffractometer (Germany). The measurement was taken in continuous mode (operated at 40 kV and 20 mA) over an angular range of 10° to 70°. The hydrodynamic mean diameter of the

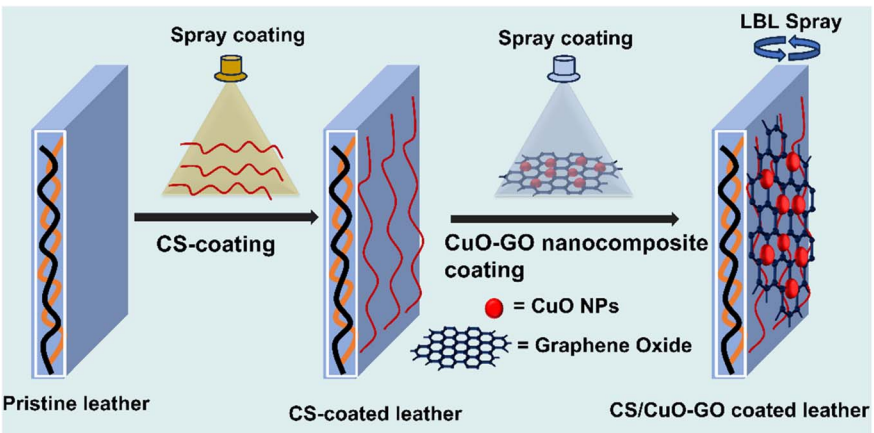

Scheme 1 Layer-by-layer assembly of CS and CuO-GO nanocomposite coating onto a leather surface.

CuO NPs was measured using a dynamic light scattering (DLS) device (Nano Partica sz-100V2 series, Horiba Scientific, Japan). Thermogravimetric analysis was carried out on a PerkinElmer 8000 TGA analyser (USA). TGA was conducted in aluminium cells with N_2 flow from room temperature to 800 °C at a rate of 10 °C min^{-1}. The contact angle was measured using a contact angle measurement device (DMe-211, Kyowa Interface Science Co., Ltd, Japan) in static conditions. The contact angle values were measured within 0–5 seconds after placing the drop.

2.7 Antibacterial activity assay of CS/CuO-GO NC coated leather

2.7.1 Zone of inhibition test (ZOI). The ZOI test was conducted following the AATCC test method 90-2011. *E. coli* and *B. subtilis* were designated as model Gram-negative and Gram-positive bacteria, respectively. Bacterial solutions with concentrations of 1×10^6 CFU mL^{-1} and 1×10^8 CFU mL^{-1} were evenly poured into 150 mL of agar solution at 50 °C. Agar solution containing the bacteria was poured into a culture dish with a volume of 30 mL. After allowing it to stand at room temperature for 10 minutes, rounded leather samples with a diameter of 6 mm were placed into the culture dish. The dish was then incubated for 24 h at 37 °C. The average width of ZOI on either side of the round sample was calculated using the following equation:[26]

$$W = (T - D)/2$$

where W = width of ZOI, mm; T = total diameter of round sample and clear zone, mm; D = diameter of the round sample, mm.

2.7.2 Bacterial killing efficiency assay of treated leather samples. A dry leather sample weighing 500 mg was washed multiple times with sterilized water, then cut into pieces and placed in a tube containing 10 mL of sterilized PBS with a bacterial concentration of 1×10^4 CFU mL^{-1}. The tubes were incubated at 37 °C with shaking at 150 rpm on an orbital shaker. At the initial time point (0 h) and 1 h, a 20 μL aliquot of the bacterial solution was taken from each tube and mixed with nutrient agar. The culture dish was held at 37 °C for 18 h. Afterwards, the colonies were counted to get the number of colony-forming units. The bacterial killing efficiency[26] is defined as:

$$\text{Killing efficiency (\%)} = (\text{cell count at 0 h} - \text{survivor cell counts at 1 h})/\text{cell count at 0 h} \times 100\%$$

To study the cyclic antibacterial properties of treated leather, samples were removed from the bacterial solution after 1 h and rinsed with sterile PBS for 10 min. This process was repeated twice more, totalling three cycles of assessment.

2.8 Release behavior of Cu^{2+} from CS/CuO-GO coated leather

The study investigated the release of copper ions from cross-linked CS/CuO-GO spray-coated leather using atomic absorption spectroscopy (AAS, PinAAcle 900H, Netherlands). A 500 mg dry leather sample was dissolved in 10 mL of a 4 : 1 mixture of concentrated nitric acid (HNO_3) and hydrogen peroxide (H_2O_2) for nitrolysis, then diluted to 100 mL with water to determine the copper content. To measure the Cu^{2+} ion release rate, another 500 mg dry leather sample was placed in 10 mL of phosphate-buffered saline (PBS, pH 7.4) and incubated at 37 °C. At specific intervals, 10 mL of solution was withdrawn and replaced with fresh PBS, and the released Cu^{2+} concentration was measured using AAS.

2.9 Mechanical tests

Mechanical tests were conducted to assess the impact of CS/CuO-GO nanocomposite coating on the leather surface. Tensile, tear strength, and stitch sear strength (Tensile tester STD 172, Soraco, Italy), and Dry & Wet Rub Fastness (SATRA, STM 421, UK) were measured according to ASTM D412c, ASTM D624, DIN 53331, and DIN 54021, respectively. The average test results were determined using the values obtained from three replicates, ensuring accuracy and reliability in our findings.

2.10 Water vapor permeability test

The water vapor permeability of materials was tested to find out the effectiveness of the nanocomposite-coated leather in case of comfort. Water vapor permeability of leather samples was conducted following the standard SATRA TM-172 using a WPV machine (SATRA STM 473, UK). The amount of water vapor that can be transmitted through a leather sample is determined by passing a desiccant air of specified humidity at a set velocity into the sample with the help of a WVP apparatus. The circular leather sample is cut into a circle with a diameter of 34 mm. First, pure silica gel was taken into a test pot and at least 2/3rd or 1/2 of it was filled. Then, the 1st weight was measured. The sample was fixed into the open end of the test pot with the grain facing the outside direction of the pot. It was kept for 8 h. Finally, the final mass of the conjugated sample was taken. The water vapor permeability of the leather sample was measured using the following formula:

$$\text{WVP} = (M_2 - M_1)/A\,(T_2 - T_1)$$

Here, M_1 = pot weight before the work, M_2 = pot weight after the vapor passed, A = area of the sample, T_2–T_1 = total time.

2.11 Porosity measurement

Porosity was determined using the liquid displacement method described in Sarker *et al.*[27] Ethanol was utilized as a displacement liquid due to its non-interference with the three-dimensional structure of the leather sample. Then, the leather samples' length, width, and height were measured with a digital calliper, followed by immersion in ethanol and centrifugation for 10 min at 1200 rpm to speed up the infiltration process. The excess ethanol was removed with filter paper, and the leather samples were weighed repeatedly until a constant mass was obtained. The analysis was performed in triplicate, and the porosity was calculated using the following formula:

$$\text{Porosity} = (W_2 - W_1)/\rho V \times 100\%$$

where W_1 and W_2 are the weight of the leather samples before and after immersion in absolute ethanol, respectively; ρ is the density of absolute ethanol and V is the volume of the leather sample.

2.12 Statistical analysis

All experimental data were done in triplicate. The experimental results are reported as means ± standard deviations values (SDs). A one-way ANOVA test was conducted for statistical analysis using Origin 9.1 to identify significant variations between triplicates. To evaluate the findings, $p \leq 0.05$ was counted as statistically significant.

3 Results and discussion

3.1 Characterization of GO, CuO NPs, and CuO-GO nanocomposites

The formation of colloidal CuO nanoparticles, GO and CuO-GO nanocomposites was evaluated by XRD, UV-visible spectroscopy, zeta potential, and TEM analyses. The hydrodynamic size of colloidal CuO NPs was analysed by DLS.

XRD analysis of GO showed that the major diffraction peak was at a 2θ angle of 10.78°, which corresponds to the (002) reflection of GO[28] and represents d-spacing of 0.81 nm higher than that of primordial graphite (0.34 nm) (Fig. 1a). The small diffraction peak at 26.7° indicates the hexagonal lattice of natural graphite.[22] The X-ray diffractogram of CuO nanoparticles is shown in Fig. S1 (ESI).† The crystal planes (−111), (111), (−202), (020), (202), (−113), and (−311) are represented by the diffraction peaks for pure CuO at 2θ angles of 35.5°, 38.68°, 48.70°, 53.36°, 58.31°, 61.5° and 65.96°, respectively. They are connected to the distinctive diffraction patterns of the CuO nanoparticle's monoclinic phase (according to the JCPDS card number 41-0254).[28,29] It was suggested that GO exfoliation might obscure the diffraction peak. The XRD pattern of the CuO-GO nanocomposite revealed 2θ angles at 35.5°, 38.68°, 48.70°, 53.36°, 58.31°, and 61.5°, which correspond to (−111), (111), (−202), (020), (202), and (−113) crystal planes, respectively.[28] It also exhibited 2θ at 10.32°, which corresponds to GO layers (Fig. 1a). As a result, the Cu ions that form a layer-on-layer network were strongly coupled with the carbonyl groups of both the carboxylic acids and ketones that were present on GO. The resultant porous 3D network enhanced the hydrophilicity of the CuO-GO nanocomposites. There were no recognizable impurity peaks present in the diffractogram.[30]

The UV-vis spectra for GO and CuO-GO NC were assessed and represented[28] in Fig. 1b. The main absorbance peak was identified at 226 nm, corresponding to π–π* transitions of C=C bonds in amorphous carbon systems. Additionally, the broad shoulder at approximately 300 nm was attributed to the n–π* transition of C=O bonds.[31] Similar results were reported by T. Tene *et al.*[32] For the CuO-GO nanocomposites, the UV-vis spectra have two unique absorption peaks at 275 and 365 nm, related to π plasmon excitation of the graphitic structure and CuO, respectively. The graphitic peak at 226 nm red-shifted to 275 nm because of the extension of conjugation. A broad band between 300 and 399 nm was obtained, ascribing the inter-band transition of central electrons of Cu metal and CuO nanocrystals. The zeta potential of CuO-GO nanocomposite was measured by DLS and depicted in Fig S2.† The zeta potential of GO is high due to the presence of negatively charged OH and COOH groups. The zeta potential value of CuO-GO was −9.5 mV at a pH of 6.8. The results indicate that the influence of negatively charged (or electron density) is lower for the nanocomposite, possibly due to the charge neutralization of GO–COO– with copper complexation.[33] The source of these negative charges is a lone pair of oxygen-containing functional groups. Further, the average size of CuO NP measured by the particle size analyzer was 11.00 nm (Fig S3†) with a narrow size distribution (PDI of 0.45). The obtained result was similar to the previous report of green synthesis of CuO NP from *Aloe vera* leaf extract.[34]

The morphological characterization of CuO, GO, and CuO-GO nanocomposite by TEM analysis is shown in the Fig. 2.

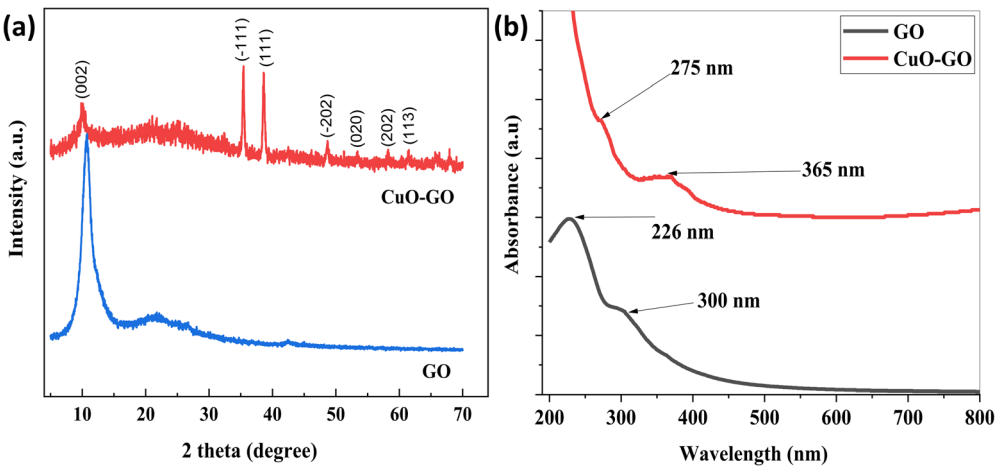

Fig. 1 (a) XRD spectra and (b) UV-visible spectra of GO and CuO-GO nanocomposites, respectively.

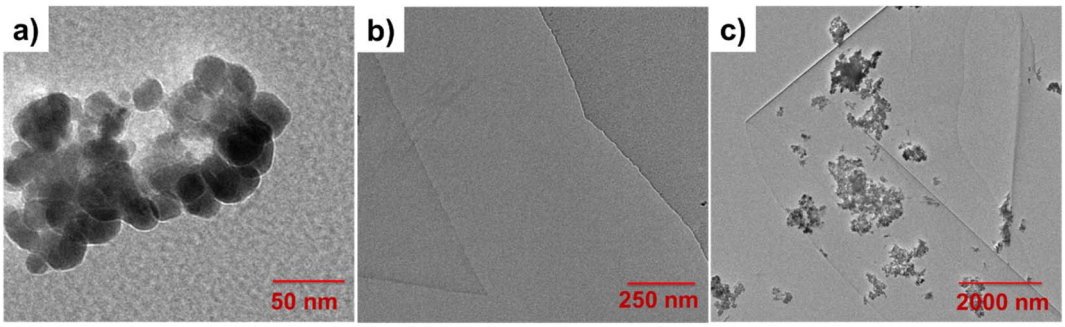

Fig. 2 TEM images of (a) CuO nanoparticles, (b) graphene oxide, and (c) CuO nanoparticles deposited onto the surface of graphene oxide.

Spherical copper oxide nanoparticles have high morphological uniformity with a size range of 30–80 nm (Fig. 2a). The presence of thin stacked flakes of forms with clearly defined multi-layered structures at the edge is confirmed by the TEM image of GO sheets (Fig. 2b).[35] A close look at the TEM images of the CuO-GO nanocomposite (Fig. 2c) reflected the existence of CuO nanospheres and revealed a uniform distribution of copper oxide NPs compared with GO sheets after the hydrothermal self-assembly process. Zhang *et al.* prepared the copper oxide–graphene oxide nanocomposite for catalytic applications and reported the homogeneous distribution of CuO nanoparticles onto GO sheets.[36]

3.2 Characterization of CS/CuO-GO nanocomposite-coated leather

The crust leather was coated by layer-by-layer assembly of CS and CuO-GO nanocomposite after complete drying of the first layer. Here, a 2 wt% of chitosan was mixed with PVA solution for proper binding with the leather surface, and two different concentrations of CuO-GO nanocomposite (1 mg mL^{-1} and 5 mg mL^{-1}) were prepared for application on the leather surface. Chitosan solution was first sprayed onto the leather surface, drying of the first layer, and a dispersion of nanocomposite was sprayed onto the chitosan-coated leather surface. This procedure was conducted two times to impart double coating on the leather surface. The tinted coating solution changed the original colour of pristine leather. Fig S4† showed the optical images of leather before and after the nanocomposite coating. Though the colour change was not prominent on black natural grain bovine leather samples, it creates a shiny and reflective surface. Various analytical methods were employed to evaluate the coated leather samples, including ATR-FTIR, FE-SEM, XPS, and TGA.

3.2.1 ATR-FTIR analysis

The ATR-FTIR spectra of CuO, GO, CuO-GO, CS, and different ratios of CS/CuO-GO nanocomposite-coated leathers are depicted in Fig. 3. The IR spectra of CuO-NPs are depicted in Fig. 3a. The spectra of CuO showed a broad peak centered at 3650–3050 cm^{-1}, which is ascribed to the stretching of O–H groups of water molecules (due to adsorbed moisture on the surface of the NPs)[28] and the stretching vibration of the C–H bond occurs at 2930 cm^{-1}. The peaks at 1560 cm^{-1} correspond to the C=O, 1400 cm^{-1} represents the C–H bond and 1055 cm^{-1} denotes the C–O bond. The peak at 660 cm^{-1} is specific to the CuO lattice structure, confirming the formation of CuO.[25] FT-IR analysis shows that the synthesis of CuO NPs is due to phytochemicals in the aqueous extract, which are responsible for reducing and stabilizing the metal ions.[37] Further, the IR spectra of GO exhibit a wide peak at 2990–

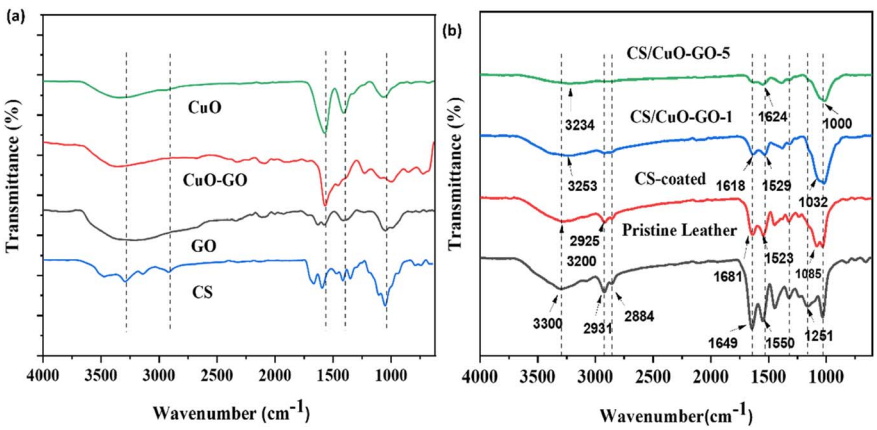

Fig. 3 ATR-FTIR spectra of (a) CuO, GO, CuO-GO, and CS, and (b) different ratios of CS/CuO-GO nanocomposite-coated leathers.

3750 cm^{-1} (representing the O–H stretching vibration of absorbed H_2O molecules), 1676 cm^{-1} (C=O stretching vibration of carboxyl and carbonyl groups), 1432 cm^{-1} (C=C stretching vibration of the aromatic ring) and 1086 cm^{-1} (C–O stretching vibration of the epoxy and alkoxy groups).[38] The ATR-IR spectra of CuO-GO nanocomposite[28] exhibited the characteristic bands of CuO and GO. The broad peaks from 2990–3750, 1676, 1432, and 1086 cm^{-1} of GO reduced after the formation of CuO-GO nanocomposite, which implies that the peaks corresponding to the C=O group and –OH group are reduced.[25] The peaks at 2920 and 2856 cm^{-1} are associated with asymmetric and symmetric $-CH_2$ groups. The peak at 592 cm^{-1} is linked to the Cu–O bond in monoclinic CuO, a specific crystalline form of copper(II) oxide. These peaks confirm the presence of monoclinic CuO in the nanocomposites.[30] The FT-IR spectrum of CS is also shown in Fig. 3a. The peaks at 3435, 1635, 1530, 1360, and 1060 cm^{-1} represent the stretching vibration of –OH and $-NH_2$ groups, the C=O group, N–H bond, C–N and bending of the N–H bond, and C–O–C glycosidic bond, respectively that forms the chitosan chain.[39]

The pristine leather showed a broad peak at 3300 cm^{-1}, representing the –OH and –NH groups of collagens (Fig. 3b). The peaks at 2931 and 2884 cm^{-1} also show the asymmetric and symmetric stretching of the C–H bond. The peak at 1649 and 1550 cm^{-1} represents the stretching of the amide I (C=O) group and amide II (N–H bending and C–N stretching), respectively.[40] Chitosan-coated leather showed peaks at 3200 cm^{-1} for –OH overlapped with –N–H and the peak at 1523 cm^{-1} corresponds to the in-plane bending vibration of the N–H bond, which are distinctive peaks of chitosan. Likewise,

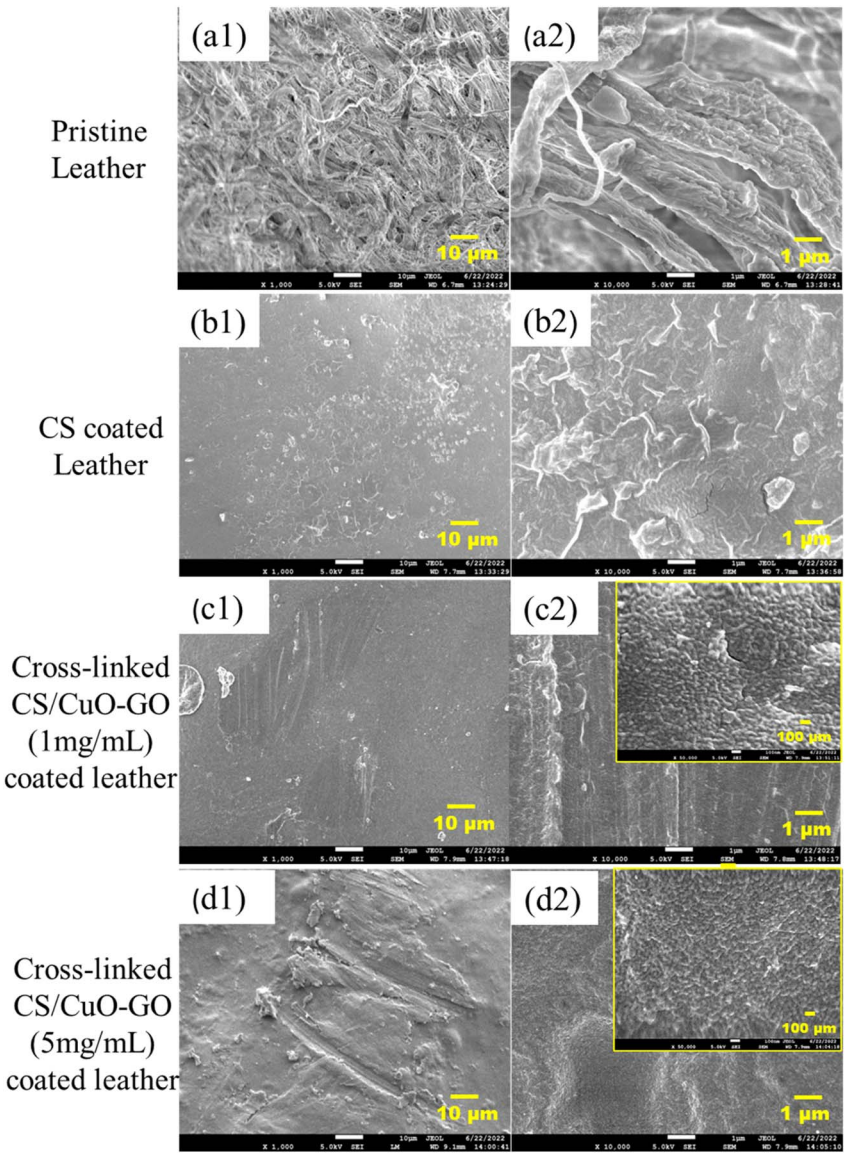

Fig. 4 FE-SEM images of pristine leather (a1 and a2), chitosan-coated leather (b1 and b2), CS/CuO-GO (1 mg mL^{-1}) coated leather (c1 and c2), and CS/CuO-GO (5 mg mL^{-1}) coated leather (d1 and d2) samples at different magnifications (1000× and 10 000×). Insets show magnified images (50 000×), indicating the presence of CuO-GO nanostructure on the leather surface.

a sharp peak at 1085 cm^{-1} was observed in the chitosan-coated leathers but absent from the pristine leather. In the case of the CS/CuO-GO-1 coated leather, the FTIR spectra showed peaks at 3253 cm^{-1}, 1618 cm^{-1}, and 1529 cm^{-1}, representing –OH group, –C═O group and N–H bending, respectively arising from CS and CuO-GO layers. The two deep peaks at 1062 and 1015 cm^{-1} represent the C–O stretching vibration of the CS/GO layer. These peaks are broader from CS-coated and pristine leather. Furthermore, the intensity of the CS/CuO-GO-5 peaks on the FTIR spectrum were lower than that of chitosan-coated leather because of the interaction between 5 mg mL^{-1} of CuO-GO nanocomposite and chitosan.

3.2.2 FE-SEM micrographs of CS/CuO-GO coated leather

The surface texture, skin pore patterns, and fibre structure of coated leathers were evaluated by FE-SEM.

As seen in the methodology, positively charged chitosan (with 5% PVA solution as a binder) and negatively charged CuO-GO nanocomposite were assembled on the leather *via* a layer-by-layer spraying process to create the CS/CuO-GO film on the grain portion of the leathers. Leather is essentially a biomass made of collagen fibres. FE-SEM provided a clear view of the collagen fibrous network structure to the immaculate leather's surface morphology (Fig. 4a1). Fig. 4a2 in its expanded form exhibits the usual cross-sectional structure of collagen fibres. The amino acid composition of collagen, which includes acidic amino acids like glutamic and aspartic acid, reveals numerous carboxyl groups on its surface.[26] Therefore, the formation of a persistent layer of cationic chitosan on the surface of leather was made possible by the electrostatic interaction among carboxyl groups and amino groups. The treated leather surface smoothed out and the voids between collagen fibres were filled following chitosan coating, as seen in Fig. 4b1 and b2. Then, a layer of CuO-GO composite with an immense concentration of carboxyl groups was uniformly placed on top of the chitosan layer. The microstructure of CuO-GO nanocomposite clusters produced by composite aggregation after drying was visible from the FE-SEM images in Fig. 4c1, c2, d1 and d2. Unsmooth and clustered leather surfaces indicate CuO-GO nanocomposite coating on leather surfaces.

3.2.3 XPS analysis of CS/CuO-GO coated leather surface

Further, the chemical state of the CS/CuO-GO nanocomposite coating was determined through XPS analysis. In pristine leather (Fig. 5a), the identification peaks are at 284.8 eV, 400 eV, and 533 eV for C 1s, N 1s, and O 1s, respectively.[26] For CS-coated leather, peaks at 533.1 eV and 531 eV correspond to O 1s for organic C–O and organic C═O bonds, respectively, the peak at 400 eV represents the C–NH_2 bond and peaks at 284.8 eV, 286 eV, and 288 eV indicate the existence of C–C, C–O–C and O–C═O bonds, respectively which confirms C 1s (Fig. 5b). Compared to pristine leather (Fig. 5a) and CS-coated leather (Fig. 5b), the survey spectrum of CuO-GO treated leather revealed the presence of Cu 2p and Cu 2s signals in Fig. 5c and e.

Furthermore, the Cu 2p core level XPS spectra of CS/CuO-GO (1 mg mL^{-1}) coated leather and CS/CuO-GO (5 mg mL^{-1}) coated leather were shown in Fig. 5d and f, respectively, in which two peaks at 932.9 eV and 952.3 eV represent Cu $2p_{3/2}$ and Cu $2p_{1/2}$. The splitting of the 2p doublet of Cu is approximately 19.6 eV.[41] All the Cu and C signals observed through XPS confirmed the construction of the external CS/CuO-GO nanocomposite layer on the leather surface where the CS/CuO-GO (5 mg mL^{-1}) layer showed higher Cu and C signals.

3.2.4 TGA of CS/CuO-GO nanocomposites coated leather

Fig. 6 illustrates the TGA thermograms of pristine leather, CS-coated leather, and CS/CuO-GO nanocomposite-coated leather. In addition, the weight loss curve of chitosan, CuO-NPs, GO, and CuO-GO was presented[28] in Fig S5.† The weight loss curve of pristine leather showed three stages of weight loss.[42] A very smooth weight loss (about 15%) was found at around 270 °C due to moisture content and confined water molecules. The primary decomposition (weight loss of about 60%) occurs between temperatures of 270 °C to 400 °C. Above 400 °C, the residual organic materials (such as remaining fats or degraded proteins) present in the leather begin to degrade. The rate of weight loss slows, but further decomposition continues until mostly inorganic ash remains.[43] In CS-coated leather, the initial weight loss due to moisture content was the same pattern as the leather sample at temperatures ranging from 30 °C to 150 °C. At temperatures between 300 °C to 700 °C, the degradation occurred due to the degradation of the polymer chains of chitosan and collagen.[44] At 700 °C, the weight loss for CS-coated leather was about 74%, while an 83% weight loss was seen in pristine leather. This thermal improvement suggests that chitosan can provide a protective barrier against heat. The CS/CuO-GO-5 nanocomposite-coated leather exhibited the highest residue at 700 °C, showing 70% weight loss. The CS/CuO-GO-1 nanocomposite-coated, CS-coated, and pristine leather samples displayed weight losses of 72%, 74%, and 83%, respectively.

This indicates that the CS/CuO-GO-5 nanocomposite-coated leather offers better thermal stability than the other samples. The CS and CuO-GO nanocomposite can easily penetrate and form a complex within the tanning agent, establishing cross-links with the network structure of collagen fibres.[45] This dense cross-link improves the thermal stability of the coated leather.[46] Again, cationic chitosan has a strong interaction with negatively charged graphene oxide, which results in the thermal stability of the composite coating onto the leather surface. Moreover, the 'torturous path' of graphene sheets improves thermal stability because of their ability to avoid oxygen infusion.[47]

3.3 Antibacterial activities of CS/CuO-GO coated leather

The antibacterial efficacy of CS/CuO-GO-coated leather surfaces was investigated using *E. coli* and *B. subtilis* as typical model bacteria (Fig. 7).

Pristine leather and chitosan-coated leather were developed as controls, and the ZOI of these leathers was initially examined. This antibacterial test was carried out for bacterial concentrations of 10^6 CFU mL^{-1} for 48 h. After being incubated with two bacterial strains, the leather coated with CS/CuO-GO nanocomposite eliminated all the germs underneath and

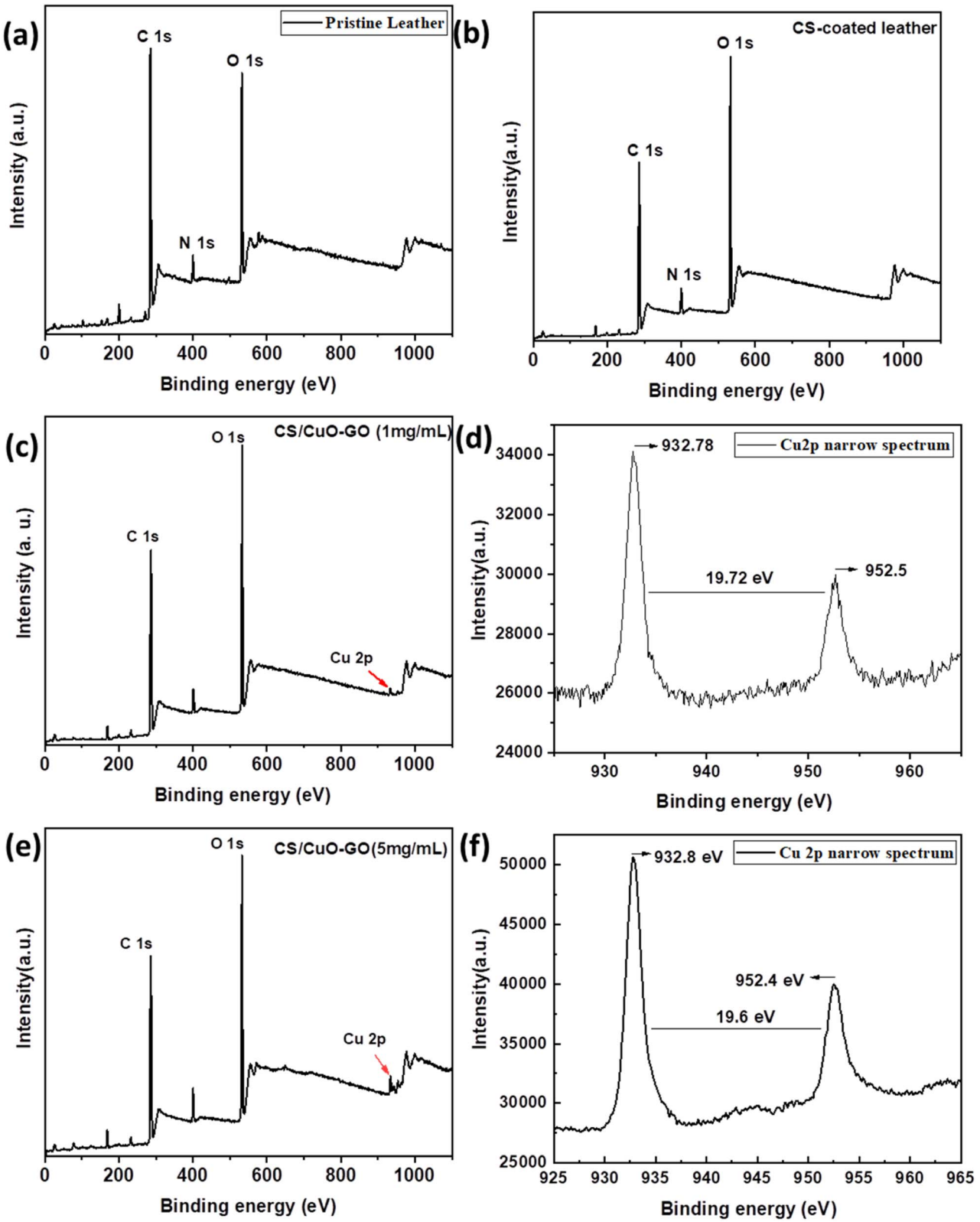

Fig. 5 XPS spectra of (a) pristine leather, (b) CS-coated leather, (c) CS/CuO-GO (1 mg mL^{-1}) coated leather, (d) Cu 2p core-level of CS/CuO-GO (1 mg mL^{-1}) coated leather, (e) CS/CuO-GO (5 mg mL^{-1}) coated leather, and (f) Cu 2p core-level of CS/CuO-GO (5 mg mL^{-1}) coated leather.

surrounding the sample (Fig. 7a and b). Additionally, the average ZOI widths of nanocomposites-coated samples were much greater than that of chitosan-coated leather samples (Fig. 7c). Further, leather coated with CS/CuO-GO-5 nanocomposite containing 5 mg mL^{-1} of CuO-GO showed a much bigger ZOI than leather coated with CS/CuO-GO-1. CS/CuO-GO

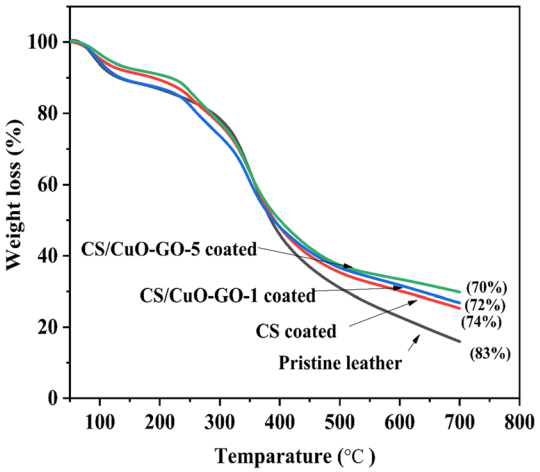

Fig. 6 TGA thermogram of pristine leather, CS-coated leather, CS/CuO-GO (1 mg mL^{-1}), and CS/CuO-GO (5 mg mL^{-1}) nanocomposite-coated leather.

coated leather showed a ZOI of about 5 ± 0.3 mm for *E. coli* and 5.5 ± 0.24 mm for *B. subtilis*. A similar ZOI was reported for CS/Ag NPs incorporated leather[26] and for ZnO NPs coated leather[48] for *E. coli* and *S. aureus*. Since the zone of inhibition increases with nanocomposite concentration, we can conclude that the antibacterial property is directly proportional to the analyte concentration used. This is because more CuO-GO nanocomposite results in more damage to bacterial cell walls and provides more effective antibacterial activity. The test was conducted with bacterial concentrations of 10^8 CFU mL^{-1} and similar results are shown in the ESI (Fig S6).†

The bacterial killing efficiency of CS/CuO-GO nanocomposite-coated leather samples was evaluated against Gram-negative and Gram-positive bacteria after repeated washing. A bacterial concentration of 10^4 CFU mL^{-1} was taken for this test.[26] After analysing the ZOI results, the killing efficacy of the prepared CS/CuO-GO nanocomposite coating was higher than that of the bare chitosan coating, reaching over 99.5% after only 1 h of growth with bacteria (Fig. 7d). The results showed that the CS/CuO-GO nanocomposite coating demonstrated significantly improved antibacterial action compared to the bare CS-coating. This improvement is attributed to the combined effects of the contact-killing mechanism of the chitosan layer and the release of Cu^{2+} ions from the CuO-GO layer, which leads to the formation of

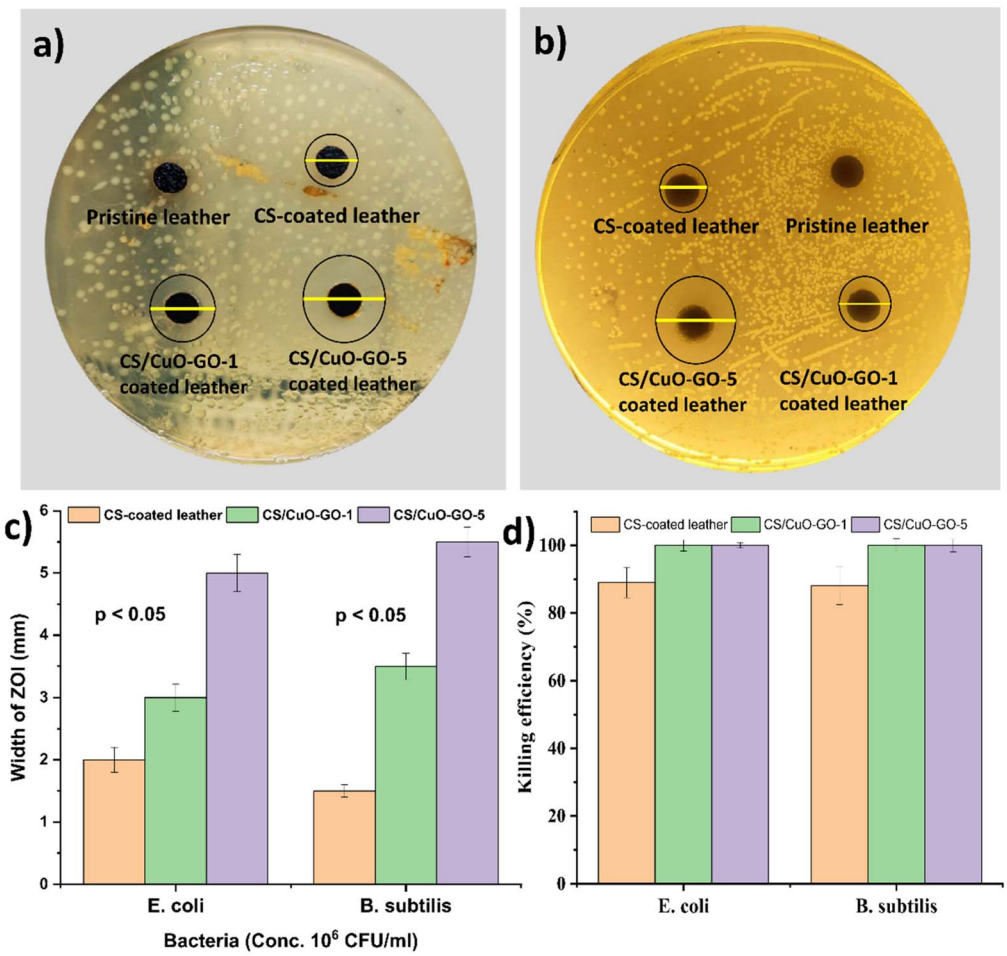

Fig. 7 ZOI of leather samples against *E. coli* (a) and *B. subtilis* (b). Average width calculated from the ZOI of each leather sample (c). Bacteria-killing efficiency of leather samples after 1 h incubation with bacteria (d). All sample areas were circled with a solid ring. Error bars represent the mean ± SD ($n \geq 3$). *P was determined by the Student's t-test.

reactive oxygen species (ROS). In addition to CS and CuO nanoparticles, GO also contributes to the antimicrobial activity.[49]

3.4 Long-acting antibacterial activity of CS/CuO-GO coated leather by accumulative release of Cu^{2+}

This test was conducted to assess the release of Cu^{2+} ions from CS/CuO-GO coated leather after repeated washing. The release factor was measured after 72 h using a shaking speed of 150 rpm at 37 °C. AAS was used to measure the Cu^{2+} release performance from the CS/CuO-GO nanocomposite-coated leather to establish the durability of the coating. When 1 g of dry CS/CuO-GO-5 coated leather was submerged in 10 mL of water after 72 h at 37 °C, the cumulative release of Cu^{2+} was around 0.9% and the copper content was around 0.01378 mg per gram of CS/CuO-GO-5 coated leather (Fig. 8). The results showed that the release of Cu^{2+} showed an incredibly persistent performance and that a covering made of nanocomposite materials may have long-lasting antibacterial properties. The result is in line with the reported Ag^{+} ion release from CS/GA@AgNP composite-coated dry leather after 72 h.[26]

The antibacterial action of CuO NPs depends on the characteristics of the bacterium cells. The antimicrobial activities of the CuO-GO nanocomposite could result from a combination of the effects of the native GO and the surface-deposited CuO NPs. The mechanism of antibacterial action of CuO-based materials may follow a variety of antibacterial processes that can work separately or together, including cellular absorption, dissolution, or formation of reaction oxide species (ROS).[50] Together, these variables have the potential to cause internal leakage, metabolic retardation, DNA destruction, protein oxidation, lipid peroxidation, and cellular membrane damage in bacterial cells. ROS causes cell lysis in bacterial cells by causing intercellular and membrane damage. Additionally, copper nanomaterials easily release dissolved ions from their outer surface while in solution. This indicates that ROS generation and ion dissolution are probably working together to provide the reported antibacterial action.

In general, there are three steps involved in the generation of antimicrobial activity for graphene-based nanomaterials. First, the nanosheets accumulate on the surface of the bacteria. Secondly, membranes are interrupted by sharp nanosheets. Finally, there is superoxide anion-independent oxidation.[18] The results of this study align with these pathways; therefore, the incremental release of Cu^{2+} ions from the leather surface coating significantly enhances the long-acting antibacterial activity.

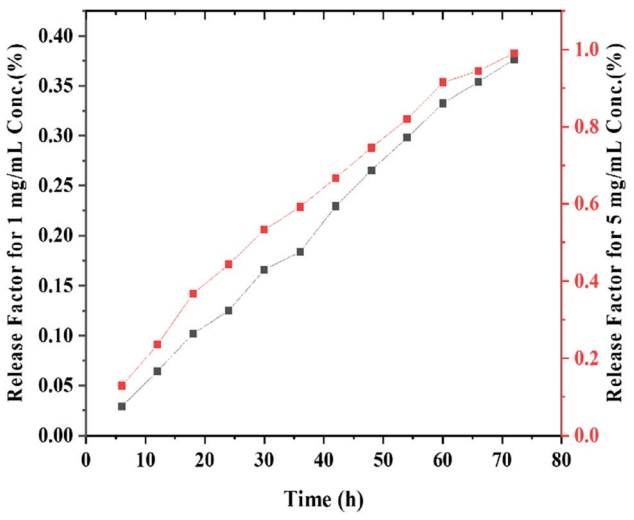

Fig. 8 Accumulative release factor of Cu^{2+} ions from CS/CuO-GO-1 and/CS/CuO-GO-5 coated leather samples.

3.5 Cyclic antibacterial activities of CS/CuO-GO coated leather

Currently, a major issue with many bactericidal coatings is that they can be easily covered by adsorbed dead microbial cells, leading to a loss of antibacterial effectiveness and potentially triggering an immune response.[51] To restore their biocidal activity, it is essential to release or remove dead bacteria from the coating. In the case of the CS/CuO-GO nanocomposite coating, the outer layer made of CuO-GO consists of a densely packed, negatively charged graphene oxide (GO) sheet. Under neutral conditions, this negatively charged layer can electrostatically repel dead bacteria.[18] Bacteria can be released from the coating surface through simple washing. To ensure that wearable leather products maintain durable antibacterial properties during everyday use, the CS/CuO-GO nanocomposite coating must preserve its effective bactericidal activity despite exposure to washing and abrasion. Therefore, the antibacterial effectiveness of the CS/CuO-GO coated leather samples was examined under cyclic washing and abrasion conditions. The investigation demonstrated the potent antibacterial properties of the CS/CuO-GO nanocomposite coating against *E. coli* and *S. aureus*, with chitosan-coated leather serving as the control. After 1 h incubation with bacteria, the leather samples were extracted from the bacterial solution and rigorously washed with sterilized phosphate-buffered saline (PBS) for 10 min. The samples were then re-incubated with bacteria for another hour, and the killing efficiencies were precisely measured, marking the completion of one cycle before the subsequent use. This study decisively tested the leather samples over three cycles in the presence of bacteria.

As the number of cycle periods increased, the killing efficiency of chitosan-coated leather against *E. coli* and *B. subtilis* eventually dropped below 90% (Fig. 9a and b). The mask effect of imbued or dead microorganisms probably contributed to this reduction of antibacterial effectiveness. In contrast, the CS/CuO-GO nanocomposite-coated leather showed better killing efficiency (>99.5%) even after three cycles. The findings showed that the CS/CuO-GO nanocomposite-coated leather could be washed with water to free any adherent or dead bacteria while still maintaining its antibacterial properties for repeated use.

The excellent antibacterial activity of the CS/CuO-GO nanocomposite coating cannot be solely attributed to the combined effects of chitosan and the CS/CuO-GO coating. Instead, it is likely due to a synergistic effect that includes the contact-killing

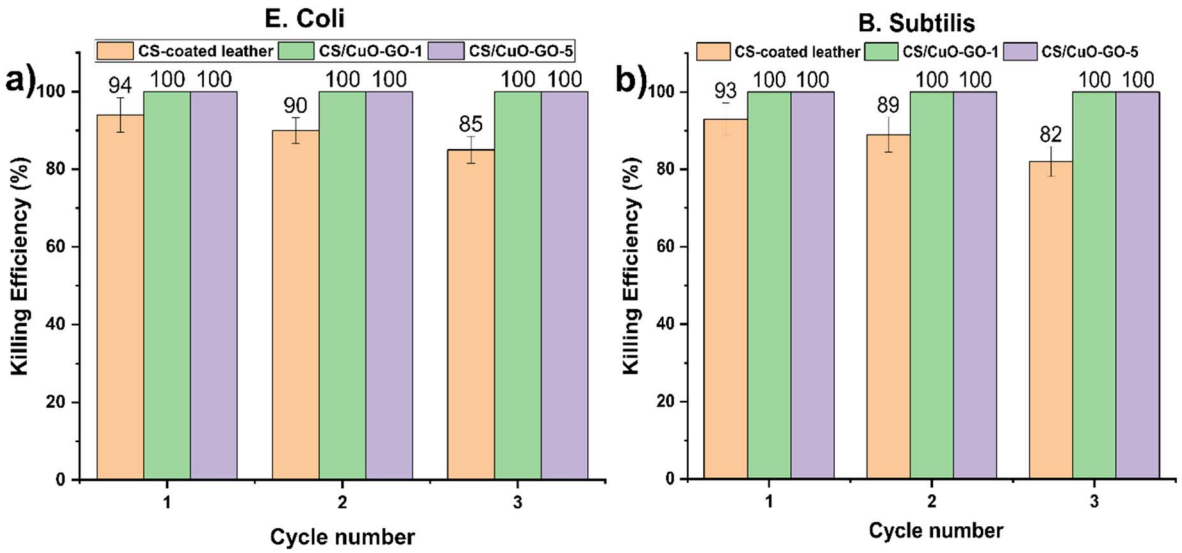

Fig. 9 Cyclic antibacterial activities of leather samples with different ratios of CS/CuO-GO coating against *E. coli* (a) and *B. subtilis* (b). Error bars represent the mean ± SD ($n \geq 3$). *P was determined by the Student's t-test, $P < 0.05$.

properties of the CS layer, the release of Cu^{2+} ions, and the bacterial-repelling characteristics of the negatively charged graphene oxide layer. Therefore, the antibacterial effect is primarily derived from the intrinsic antibacterial activity of the CuO NPs. GO also provides antibacterial properties, but the GO serves as a scaffolding framework. The water contact angle of the CS/CuO-GO nanocomposite coating was measured at 78°, which is significantly lower than the 110° observed for the CS coating (Fig. 11b). This decrease is attributed to the presence of anionic and hydrophilic oxygen-containing groups (such as carboxyl and epoxy functional groups) from the GO component. Consequently, when bacteria attach to the surface, they are killed due to the combined effects of the contact-active properties of chitosan and the release of Cu^{2+} ions. Once the bacteria are dead, they can be easily removed or repelled by the electrostatic repulsion between the negatively charged GO interface and the anionic cell membranes of the dead bacteria, resulting in a self-defensive mechanism based on the kill-and-release strategy.[26]

3.6 Mechanical properties of CS/CuO-GO coated leather

Tensile and tear strength tests were performed to evaluate whether the application of chitosan coating and inorganic CuO-GO nanocomposites could alter the physical properties of leathers (Fig. 10), which could affect their quality and compliance with some standard requirements for certain types of footwear and garments.

Fig. 10a depicts the tensile strength and % of elongation at break values corresponding to pristine leather, chitosan, and

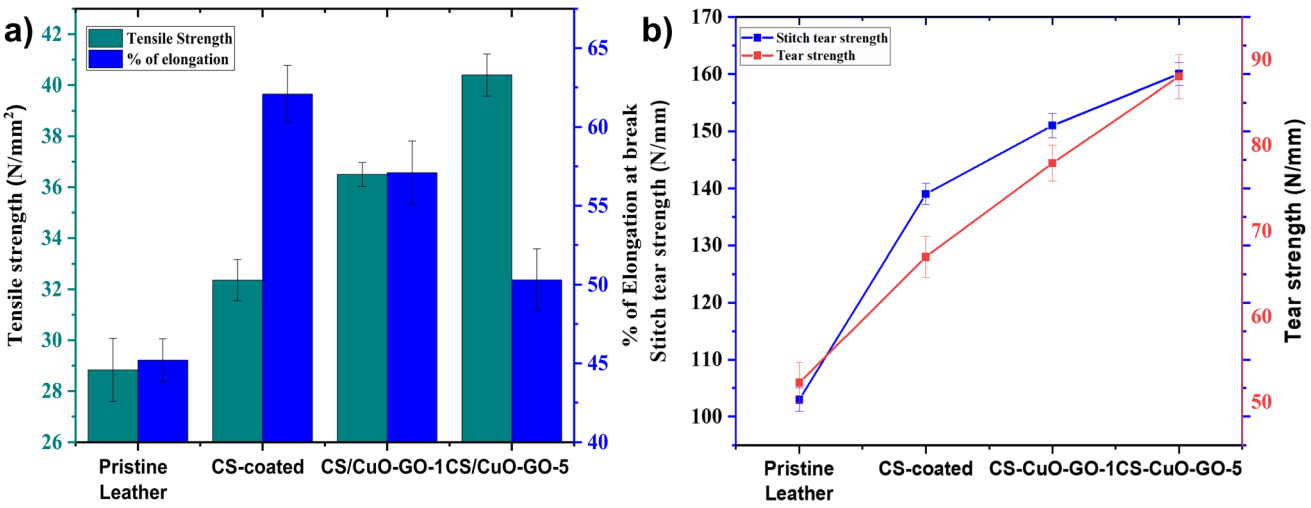

Fig. 10 Tensile strength and % of elongation at break (a) and stitch tear strength and tear strength (b) of pristine leather, chitosan-coated, CS/GO-CuO-1 (1 mg mL^{-1}) coated and CS/GO-CuO-5 (5 mg mL^{-1}) coated leather samples.

CS/CuO-GO nanocomposite-coated leather. The tensile strength of pristine and chitosan-coated leather was 28.5 and 33.5 N mm^{-2}, respectively. However, the tensile strength of CS/CuO-GO coated leather increased by about 28% to 36.5 N mm^{-2} after coating with 1 mg mL^{-1} of CuO-GO. Further, the leather coated with 5 mg mL^{-1} of CuO-GO showed a 42% increase in tensile strength. The results revealed a significant increase in tensile strength upon application of CS/CuO-GO coating on the pristine leather. Again, all the coated leathers satisfied the minimum requirements of tensile property. Therefore, a synergistic effect is achieved through the combination of three coating constituents, resulting in improved physical properties.

The uniform dispersion of CuO-GO nanocomposite in the CS layer allows for the unhindered mobility of the CS chain segment and forms a strong interface between CS and CuO-GO that can tolerate extreme stress. Moreover, GO in the CuO-GO layer can serve as a filler because of its large specific surface area and excellent mechanical properties, enhancing the overall mechanical characteristics of the applied materials. Again, the increased strength can be attributed to the effective sealing of the pores of the hair follicles of leather using nanocomposite coating, which strengthens leather fibres[52]

To ensure the desired characteristics, the percentage of elongation of the shoe upper should be within the range of 30–40%. All leathers exceeded the required limit value of 30–40% for elongation at break. The CS/CuO-GO-5 leather exhibited the lowest value among the coated leathers and was extremely close to the required limit value. Likewise, the volume of applied CuO-GO nanocomposite directly contributed to the reduction of elongation at break. The intensification of the CuO-GO nanocomposite in the coated film revealed the interface effect and stress effect between the stiff CuO-GO and CS polymer matrix. Therefore, the coating is easier to break and the elongation at break decreases.

Further, the stitch tear strengths of the prepared leather samples were conducted to assess the fibre strength of the weak region. The stitch tear and tear strength of the CS/CuO-GO nanocomposite-coated leather are shown in Fig. 10b. The required values for stitch tear strength and tear strength of the shoe upper leather are 80 N mm^{-1} (min) and 30 N mm^{-1} (min), respectively.[53] All the coated leathers surpassed the minimum values for stitch tear and tear strength, achieving peak values of approximately 160 N mm^{-1} and 90 N mm^{-1}, respectively for CS/CuO-GO-5 coated leather.

Chitosan can interact with the collagen fibre and forms complexes through electrostatic interaction among $-NH_2$ functional groups of chitosan and –COOH functional groups of collagen from leather.[54] The incorporation of CuO-GO into the CS-coated leather enhances the mechanical properties, primarily attributed to the effective dispersion of graphene oxide at the molecular level and the formation of robust H-bonds between CS and the GO surface. Additionally, the unidirectional dispersion of GO and enhanced interfacial adhesion significantly increased the mechanical properties of the nanocomposites.[55]

3.7 Dry and wet rub fastness test

The dry and wet rub fastness test was conducted to estimate the properties of the CS/CuO-GO nanocomposite-coated leather. It measures how much leather discolors due to factors like friction, water, and sweat. It is a crucial quality indicator for leather coating during use or processing. The test was conducted according to DIN 54021 standards (1024 rubs in dry and 512 rubs in wet condition).

The pristine leather treated with chitosan and CuO-GO nanocomposite has shown better dry and wet rub fastness than the control sample (Table 1). All CS/CuO-GO nanocomposite-coated leathers exhibited improved ratings, falling within the required grey scale range of 5 to 3. However, a slight decrease in the depth of shade and change in hue was found around 4/5 in wet rub fastness.

It appears that the color fastness property of the coated leather samples has increased due to the application of CS/CuO-GO nanocomposite coating. The cotton felt applied for pristine leather showed slight coloration after the dry fastness test, whereas no such coloration was observed on the CS and CS/CuO-GO coated leathers. Similar results were obtained for the wet rub fastness test, showing satisfying wear resistance provided by layer-by-layer (LBL) spray coating.[56]

The dry and wet rub fastness for both colour changing and staining was improved by one grade after layer-by-layer coating of CS and CS/CuO-GO nanocomposites (Table 1). The primary reason for this improved wear resistance would be the excellent film-forming and adsorption properties of CS/CuO-GO nanocomposites, as well as GO's lubricating ability between the substrates and the friction media due to its 2D structure.[11] The film formed by CuO-GO coating would form a rough structure, effectively resisting contact between the sample and the coating

Table 1 Dry and wet rub fastness test of treated and untreated leather samples; grey scale rating

	Dry rub fastness test				Wet rub fastness test	
Samples	Color changing (leather)		Staining on the cotton felt		Color changing (leather)	Staining on cotton felt
Cycle	512	1024	512	1024	512	512
Pristine leather	4/5	4	4/5	3	3/4	3
CS-coated	5	5	5	5	4/5	4
CS/CuO-GO (1 mg mL^{-1})	5	5	5	5	4/5	4
CS/CuO-GO (5 mg mL^{-1})	5	5	5	5	4/5	4

film during rubbing. Gao *et al.*[56] reported comparable findings after coating the leather samples with nano-SiO_2 particles. Thus, it is expected there was sufficient binding between the leather surfaces and coating materials, which did not negatively affect the rub fastness.

3.8 Water vapor permeability, porosity and water contact angle test of CS/CuO-GO coated leather

The assessment of WVP for leather samples is associated with their comfortable wearing properties. This property definitively facilitates the movement of water vapor from areas of higher humidity to those with lower humidity, primarily relying on the leather's porosity. Water is transferred through the hydrophilic groups of collagens at a specific vapor pressure. The water vapor permeability of the leather decreases after the finishing process.[47] The application of polymer nanocomposite enhances the water vapor barrier properties of leather. For shoe lining leather, it is mandatory to become water vapor permeable for the comfort of the user. Water vapor permeability is significantly influenced by the porous structure and the material's polarity.[57] The standard water vapor permeability for shoe upper leather is 0.8 mg cm^{-2} h^{-1}.[58]

The coatings of different compositions had an obvious effect on the coated leather samples. The WVP of pristine and chitosan-coated leather was 13.75 and 12.5 mg cm^{-2} h^{-1}, whereas that of CS/CuO-GO coated leather samples showed 12 and 11.5 mg cm^{-2} h^{-1} (Fig. 11a). The results indicate that the water vapor permeability (WVP) of the CS/CuO-GO coated leather exhibited a slight decline compared to the pristine leather following the coating process, although their values remained significantly higher than the standard limit. Pristine leather showed higher WVP than the finished one due to its natural, highly porous structure. The application of CS/CuO-GO-1 and CS/CuO-GO-5 nanocomposite coatings resulted in a slight reduction of WVP of leather by about 13% and 16%, respectively. This is because the WVP decreased due to the blockage of pores and hair follicles of the coated material when the nanocomposite coating was applied to the leather samples.

Table 2 Porosities of four different leather samples

Sample	Porosity (%)
Pristine leather	53 ± 3.4
CS-coated leather	43.4 ± 4.1
CS/CuO-GO-1 coated leather	27.5 ± 2.8
CS/CuO-GO-5 coated leather	14 ± 3.2

This phenomenon was confirmed by the SEM images (Fig. 4). The WVP property of the CS/CuO-GO nanocomposite coated leathers was within the permissible value instead of blocking leather pores due to coating. This is primarily due to the hydrophilic properties of coating components, which facilitate the movement of water vapor molecules. The LBL spraying method shows promise as an effective technique for creating "breathable" coatings. Table 2 shows the values obtained for porosity of CS/CuO-GO nanocomposite coated leather samples by ethanol infiltration method. The porosity of CS/CuO-GO nanocomposite coated leather samples is a crucial characteristic for their application, as it determines the moisture vapor permeability. The leather samples presented a lower porosity value with a higher coating material. This observation supports the results obtained from the WVP measurements of the leather samples.

The hydrophilic nature of the coating components was further investigated by a water contact angle test of pristine leather, CS-coated, and CS/CuO-GO-coated leather samples (Fig. 11b). Pristine leather has a WCA of 91.2° ± 1.9°, whereas the leather surface becomes slightly hydrophobic after coating with CS, with a WCA of 110° ± 2.5°. The CS/CuO-GO-1 and CS/CuO-GO-5 coated leather samples showed WCA of 71° ± 1.5° and 78° ± 2.3°, respectively. This result stems from the hydrophilic and negatively charged carboxyl groups inherent in the GO molecule. When they adhere, bacteria are killed by the combined action of chitosan's contact-active and the release of Cu^{2+} ions. The kill-release strategy produces a self-defensive function, wherein the dead microorganisms can simply be

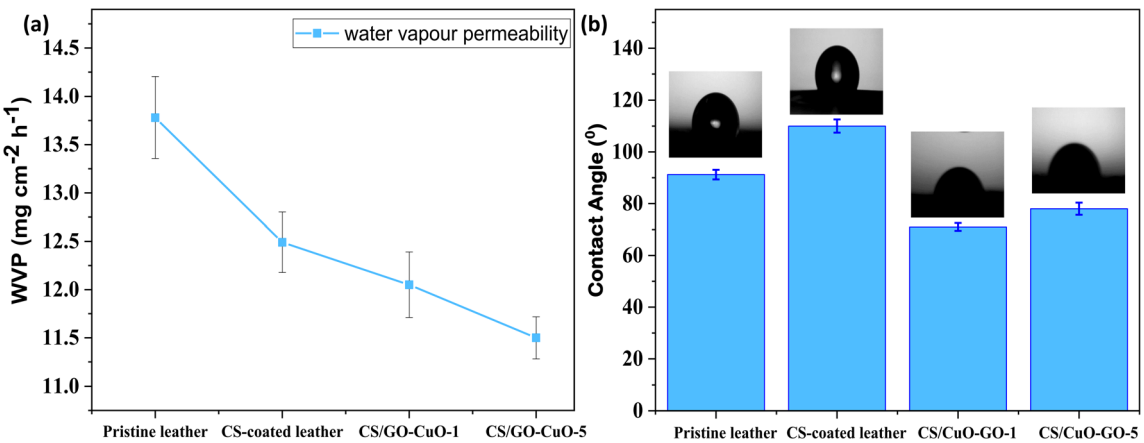

Fig. 11 (a) Water vapor permeability and (b) contact angle of pristine, CS coated, CS/CuO-GO-1 coated, and CS/CuO-GO-5 coated leather samples.

removed or repelled by the electrostatic repulsion among the negative GO interface and the negatively charged cell membrane of bacteria.[22]

Because of the existence of hydrophilic areas on pristine leather, the contact angle was lowest compared to the coated leather. After applying CS, the roughness of the coated sample increased (as observed from the SEM image in Fig. 4b), which ultimately increased the contact angle. However, the contact angle decreased again after applying CuO-GO nanocomposite coating on the CS-coated leather because of the presence of oxygen-containing moieties of GO.[59] Meanwhile, an increase in the amount of CuO-GO from 1 to 5 g mL^{-1} resulted in a slight increase in contact angle. This can be attributed to a decrease in porosity at higher concentrations, a phenomenon confirmed by the WVP and SEM investigation.

4 Conclusions

Aloe vera stabilized CuO decorated GO nanostructure was prepared *in situ*. The XRD and TEM analyses confirmed the presence of CuO nanoparticle in the GO nanosheets. A nanocomposite coating was effectively applied to the leather surface through a precise layer-by-layer assembly of cationic chitosan and anionic CuO-GO layers, followed by a durable immobilization process *via* cross-linking. These chitosan/CuO-GO nanocomposite coatings serve as a highly effective, waterborne and environmentally friendly coating that delivers outstanding antibacterial activity against both Gram-positive and Gram-negative bacteria through a powerful "kill-release" mechanism. This effectiveness is attributed to the combined effects of the contact-killing properties of the chitosan layer, the release of Cu^{2+} ions, and the bacterial-repelling characteristics of the negatively charged CuO-GO layer. Additionally, the dead cells can be removed from the coating during laundry, allowing the chitosan/CuO-GO coating to be reused while maintaining its antimicrobial activity. The cross-linked chitosan/CuO-GO nanocomposite coating significantly enhances their durable antibacterial activity and stability against laundry and colour fastness. The chitosan/CuO-GO coating incorporates bacteria resistance, bactericidal effects, and bacteria release strategies into a single system, making it promising for leather products and scale-up industrial manufacturing.

Data availability

The data supporting this article have been included as part of the ESI.†

Author contributions

Khandaker Tanzim Rahman: writing – original draft, investigation, formal analysis, and data curation. Md. Nur-E. Alam: writing – original draft, investigation, formal analysis, and data curation. M. Nuruzzaman Khan: conceptualization, investigation, methodology, data analyses, resources, writing – original draft, & editing, and project supervision.

Conflicts of interest

The authors declare that they have no known competing financial interests or personal relationships that could have appeared to influence the work reported in this paper.

Acknowledgements

M. Nuruzzaman Khan is grateful to the University of Dhaka, Bangladesh (reg/prosha-3/74252) for funding support. Khandaker Tanzim Rahman thanks the NST fellowship from the Ministry of Science and Technology, Bangladesh.

References

1 C. Cheng, J. Zhang, S. Li, Y. Xia, C. Nie, Z. Shi, *et al.*, A Water-Processable and Bioactive Multivalent Graphene Nanoink for Highly Flexible Bioelectronic Films and Nanofibers, *Adv. Mater.*, 2018, **30**(5), 1705452.

2 H. E. Emam, N. S. El-Hawary, H. M. Mashaly and H. B. Ahmed, Involvement of silver and palladium with red peanuts skin extract for cotton functionalization, *Sci. Rep.*, 2023, **13**(1), 16131.

3 H. E. Emam, R. M. Abdelhameed and H. B. Ahmed, Multi-finished protective viscose textile *via* infrared assisted one-pot incorporation of Ce-organic framework, *Cellulose*, 2024, **31**(11), 7015–7030.

4 H. E. Emam, T. Hamouda, E.-A. M. Emam, O. M. Darwesh and H. B. Ahmed, Nano-scaled polyacrylonitrile for industrialization of nanofibers with photoluminescence and microbicide performance, *Sci. Rep.*, 2024, **14**(1), 7926.

5 H. B. Ahmed, N. S. El-Hawary, H. M. Mashaly and H. E. Emam, End-to-End surface manipulation of dyed silk for perfection of coloration, UV-resistance and biocidal performance, *J. Mol. Struct.*, 2024, **1305**, 137766.

6 H. E. Emam, S. Zaghloul and H. B. Ahmed, Full ultraviolet shielding potency of highly durable cotton *via* self-implantation of palladium nanoclusters, *Cellulose*, 2022, **29**(8), 4787–4804.

7 H. E. Emam, M. H. El-Rafie and M. Rehan, Functionalization of Unbleached Flax Fibers by Direct Integration of Nano-silver through Internal and External Reduction, *Fibers Polym.*, 2021, **22**(11), 3014–3024.

8 H. B. Ahmed, K. M. Abualnaja, R. Y. Ghareeb, A. A. Ibrahim, N. R. Abdelsalam and H. E. Emam, Technical textiles modified with immobilized carbon dots synthesized with infrared assistance, *J. Colloid Interface Sci.*, 2021, **604**, 15–29.

9 A. I. Ribeiro, A. M. Dias and A. Zille, Synergistic Effects Between Metal Nanoparticles and Commercial Antimicrobial Agents: A Review, *ACS Appl. Nano Mater.*, 2022, **5**(3), 3030–3064, DOI: **10.1021/acsanm.1c03891**.

10 T. Abou Elmaaty, K. Sayed-Ahmed, R. Mohamed Ali, K. El-Khodary and S. A. Abdeldayem, Simultaneous Sonochemical Coloration and Antibacterial Functionalization of Leather with Selenium Nanoparticles (SeNPs), *Polymers*, 2021, **14**(1), 74. Available from: **https://www.mdpi.com/2073-4360/14/1/74**.

11 P. Gui, W. Long, X. Cai, Y. Yin, W. Wang and P. Wang, Influence analysis of lubrication and friction reduction of graphene oxide lubricant at SiC interface, *Colloids Surf., A*, 2024, **691**, 133897. Available from: https://linkinghub.elsevier.com/retrieve/pii/S0927775724007581.

12 W. Yu, L. Sisi, Y. Haiyan and L. Jie, Progress in the functional modification of graphene/graphene oxide: A review, *RSC Adv.*, 2020, **10**(26), 15328–15345.

13 M. Sun and J. Li, Graphene oxide membranes: Functional structures, preparation and environmental applications, *Nano Today*, 2018, **20**, 121–137.

14 M. B. Kale, Z. Luo, X. Zhang, D. Dhamodharan, N. Divakaran, S. Mubarak, *et al.*, Waterborne polyurethane/graphene oxide-silica nanocomposites with improved mechanical and thermal properties for leather coatings using screen printing, *Polymers*, 2019, **170**, 43–53, DOI: 10.1016/j.polymer.2019.02.055.

15 A. Gautam, H. Dabral, A. Singh, S. Tyagi, N. Tyagi, D. Srivastava, *et al.*, Graphene-based metal/metal oxide nanocomposites as potential antibacterial agents: a mini-review, *Biomater. Sci.*, 2024, **12**(18), 4630–4649. Available from: https://xlink.rsc.org/?DOI=D4BM00796D.

16 Q. Xia, X. Wang, Z. Huang, L. Chen, C. Li, G. Lv, *et al.*, Reduced Graphene Oxide/Titanium Dioxide Nanocomposites *via* Atomic Layer Deposition for Microwave Absorption, *ACS Appl. Nano Mater.*, 2024, **7**(14), 16864–16873, DOI: 10.1021/acsanm.4c02872.

17 G. Ungur and J. Hrůza, Influence of copper oxide on the formation of polyurethane nanofibers *via* electrospinning, *Fibers Polym.*, 2015, **16**(3), 621–628.

18 K. Biswas, Y. K. Mohanta, A. K. Mishra, A. G. Al-Sehemi, M. Pannipara, A. Sett, *et al.*, Wet chemical development of CuO/GO nanocomposites: its augmented antimicrobial, antioxidant, and anticancerous activity, *J. Mater. Sci. Mater. Med.*, 2021, **32**(12), 151.

19 Q. Liu, W. Li, H. Wang, B. M. Z. Newby, F. Cheng and L. Liu, Amino Acid-Based Zwitterionic Polymer Surfaces Highly Resist Long-Term Bacterial Adhesion, *Langmuir*, 2016, **32**(31), 7866–7874.

20 D. Mitra, M. Li, R. Wang, Z. Tang, E. T. Kang and K. G. Neoh, Scalable Aqueous-Based Process for Coating Polymer and Metal Substrates with Stable Quaternized Chitosan Antibacterial Coatings, *Ind. Eng. Chem. Res.*, 2016, **55**(36), 9603–9613.

21 A. S. Imbia, A. Ounkaew, X. Mao, H. Zeng, Y. Liu and R. Narain, Mussel-Inspired Polymer-Based Coating Technology for Antifouling and Antibacterial Properties, *Langmuir*, 2024, **40**(21), 10957–10965, DOI: 10.1021/acs.langmuir.4c00326.

22 G. Liu, K. Li, Q. Luo, H. Wang and Z. Zhang, PEGylated chitosan protected silver nanoparticles as water-borne coating for leather with antibacterial property, *J. Colloid Interface Sci.*, 2017, **490**, 642–651.

23 D. C. Marcano, D. V. Kosynkin, J. M. Berlin, A. Sinitskii, Z. Sun, A. Slesarev, *et al.*, Improved Synthesis of Graphene Oxide, *ACS Nano*, 2010, **4**(8), 4806–4814, DOI: 10.1021/nn1006368.

24 T. P. Saruchi and V. Kumar, Kinetics and thermodynamic studies for removal of methylene blue dye by biosynthesize copper oxide nanoparticles and its antibacterial activity, *J. Environ. Health Sci. Eng.*, 2019, **17**(1), 367–376.

25 F. Anjum, M. Shaban, M. Ismail, S. Gul, E. M. Bakhsh, M. A. Khan, *et al.*, Novel Synthesis of CuO/GO Nanocomposites and Their Photocatalytic Potential in the Degradation of Hazardous Industrial Effluents, *ACS Omega*, 2023, **8**(20), 17667–17681.

26 J. Xiang, L. Ma, H. Su, J. Xiong, K. Li, Q. Xia, *et al.*, Layer-by-layer assembly of antibacterial composite coating for leather with cross-link enhanced durability against laundry and abrasion, *Appl. Surf. Sci.*, 2018, **458**(May), 978–987.

27 B. Sarker, W. Li, K. Zheng, R. Detsch and A. R. Boccaccini, Designing Porous Bone Tissue Engineering Scaffolds with Enhanced Mechanical Properties from Composite Hydrogels Composed of Modified Alginate, Gelatin, and Bioactive Glass, *ACS Biomater. Sci. Eng.*, 2016, **2**(12), 2240–2254.

28 T. Siddike Moin, M. Rani Sarkar, M. F. Mahmud Chowdhury, M. M. Rahman and M. N. Khan, Electrospun Polyvinyl alcohol/Chitosan Nanofibers embedded with CuO-GO nanocomposite for pH-sensitive adsorption of Heavy Metal ions and Organic Dyes, *ACS Omega*, 2025, DOI: 10.1021/acsomega.4c08836.

29 P. P. N. V. Kumar, U. Shameem, P. Kollu, R. L. Kalyani and S. V. N. Pammi, Green Synthesis of Copper Oxide Nanoparticles Using Aloe vera Leaf Extract and Its Antibacterial Activity Against Fish Bacterial Pathogens, *Bionanoscience*, 2015, **5**(3), 135–139.

30 G. Kavith, J. V. Kumar, N. Abirami, R. Arulmozhi, R. Siranjeevi and R. Satish, Green synthesis of Copper oxide nanoparticles decorated with graphene oxide for anticancer activity and catalytic applications, *Arabian J. Chem.*, 2020, 6802–6814.

31 Y. Shen, S. Zhang, Y. Sun, C. Hai, X. Li, J. Zeng, X. Ren and Y. Zhou, Structure and Property Evolution of Graphene Oxide Sheets during Low-Temperature Reduction on a Solid Substrate, *J. Phys. Chem. C*, 2020, **124**(26), 14371–14379.

32 T. Tene, M. Guevara, F. Palacios, T. Barrionuevo, C. Vacacela Gomez and S. Bellucci, Optical properties of graphene oxide, *Front. Chem.*, 2023, **11**, 1214072.

33 S. Sulthana, A. Bhatti, E. Mathew, S. H. Quazi, N. N. Gaudreault, R. DeLong, *et al.*, Synthetic graphene–copper nanocomposites interact with the hACE-2 enzyme and inhibit its biochemical activity, *Nanoscale Adv.*, 2024, **6**(1), 188–196. Available from: https://xlink.rsc.org/?DOI=D3NA00468F.

34 S. Jabeen, V. U. Siddiqui, S. Bala, N. Mishra, A. Mishra, R. Lawrence, *et al.*, Biogenic Synthesis of Copper Oxide Nanoparticles from Aloe vera : Antibacterial Activity, Molecular Docking, and Photocatalytic Dye Degradation, *ACS Omega*, 2024, **9**(28), 30190–30204, DOI: 10.1021/acsomega.3c10179.

35 P. B. Sreelekshmi, R. R. Pillai, B. Binish and A. P. Meera, Enhanced Photocatalytic Degradation of Malachite Green

Using Highly Efficient Copper Oxide/Graphene Oxide Nanocomposites, *Top. Catal.*, 2022, **65**(19–20), 1885–1898, DOI: 10.1007/s11244-022-01693-4.

36 K. Zhang, J. M. Suh, T. H. Lee, J. H. Cha, J.-W. Choi, H. W. Jang, *et al.*, Copper oxide–graphene oxide nanocomposite: efficient catalyst for hydrogenation of nitroaromatics in water, *Nano Convergence*, 2019, **6**(1), 6, DOI: 10.1186/s40580-019-0176-3.

37 S. Jabeen, V. U. Siddiqui, S. Bala, N. Mishra, A. Mishra, R. Lawrence, *et al.*, Biogenic Synthesis of Copper Oxide Nanoparticles from Aloe vera : Antibacterial Activity, Molecular Docking, and Photocatalytic Dye Degradation, *ACS Omega*, 2024, **9**(28), 30190–30204.

38 P. Das, S. Ibrahim, K. Chakraborty, S. Ghosh and T. Pal, Stepwise reduction of graphene oxide and studies on defect-controlled physical properties, *Sci. Rep.*, 2024, **14**(1), 1–10.

39 M. N. Khan, M. T. Arafat, T. U. Rashid, P. Haque and M. M. Rahman, Chitosan-Stabilized CuO Nanostructure-Functionalized UV-Crosslinked PVA/Chitosan Electrospun Membrane as Enhanced Wound Dressing, *ACS Appl. Bio Mater.*, 2024, **7**(2), 961–976, DOI: 10.1021/acsabm.3c00958.

40 M. Arkas, G. Kythreoti, E. P. Favvas, K. Giannakopoulos, N. Mouti, M. Arvanitopoulou, *et al.*, Hydrophilic Antimicrobial Coatings for Medical Leathers from Silica-Dendritic Polymer-Silver Nanoparticle Composite Xerogels, *Textiles*, 2022, **2**(3), 464–485.

41 Z. Jin, C. Liu, K. Qi and X. Cui, Photo-reduced Cu/CuO nanoclusters on TiO 2 nanotube arrays as highly efficient and reusable catalyst, *Sci. Rep.*, 2017, **7**, 39695.

42 E. Bañón, A. Marcilla, A. N. García, P. Martínez and M. León, Kinetic model of the thermal pyrolysis of chrome tanned leather treated with NaOH under different conditions using thermogravimetric analysis, *Waste Manag.*, 2016, **48**, 285–299. Available from: https://linkinghub.elsevier.com/retrieve/pii/S0956053X15301616.

43 O. Mohamed, H. Elsayed, R. Attia, A. Haroun and N. El-Sayed, Preparation of acrylic silicon dioxide nanoparticles as a binder for leather finishing, *Adv. Polym. Technol.*, 2018, **37**(8), 3276–3286.

44 J. Liu, Y. Liu, E. M. Brown, Z. Ma and C.-K. Liu, Fabrication of Composite Films Based on Chitosan and Vegetable-Tanned Collagen Fibers Crosslinked with Genipin, *J. Am. Leather Chem. Assoc.*, 2021, **116**(10), 345–358.

45 L. Muthukrishnan, Nanotechnology for cleaner leather production: a review, *Environ. Chem. Lett.*, 2021, **19**(3), 2527–2549, DOI: 10.1007/s10311-020-01172-w.

46 H. Elsayed, M. Hasanin and M. Rehan, Enhancement of multifunctional properties of leather surface decorated with silver nanoparticles (Ag NPs), *J. Mol. Struct.*, 2021, **1234**, 130130. Available from: https://linkinghub.elsevier.com/retrieve/pii/S0022286021002611.

47 H. Elsayed, R. Attia, O. Mohamed, A. Haroun and N. El-Sayed, Preparation of polyurethane silicon oxide nanomaterials as a binder in leather finishing, *Fibers Polym.*, 2018, **19**(4), 832–842.

48 R. Saha, K. Subramani, S. A. K. Petchi Muthu Raju, S. Rangaraj and R. Venkatachalam, Psidium Guajava Leaf Extract-Mediated Synthesis of ZnO Nanoparticles under Different Processing Parameters for Hydrophobic and Antibacterial Finishing over Cotton Fabrics, *Prog. Org. Coat.*, 2018, **124**, 80–91.

49 O. Akhavan and E. Ghaderi, Toxicity of graphene and graphene oxide nanowalls against bacteria, *ACS Nano*, 2010, **4**(10), 5731–5736.

50 A. Elbourne, V. K. Truong, S. Cheeseman, P. Rajapaksha, S. Gangadoo, J. Chapman, *et al.*, The use of nanomaterials for the mitigation of pathogenic biofilm formation, *Methods in Microbiology*, Elsevier Ltd, 1st edn, 2019, vol. 46, pp. 61–92.

51 T. Chen, C. Situ, H. Huang, K. Liang, L. Zhao, Z. Wang, *et al.*, Smart Copolymer Surface Derived from Geminized Cationic Amphiphilic Polymers for Reversibly Switchable Bactericidal and Self-Cleaning Abilities, *Langmuir*, 2023, **39**(30), 10521–10529, DOI: 10.1021/acs.langmuir.3c01005.

52 J. Ma, N. Yang, W. Li, Y. Zhou and X. Sun, Functional nanocomposite based on waterborne polyurethane and layered double hydroxide as a flame retardant for leather, *J. Cleaner Prod.*, 2022, **380**, 134966. Available from: https://linkinghub.elsevier.com/retrieve/pii/S0959652622045395.

53 S. Dutta, *Introduction To The Physical Testing Of Leather*.

54 Q. Fan, J. Ma, Q. Xu and W. An, Progress in Organic Coatings Multifunctional coatings crafted *via* layer-by-layer spraying method, *Prog. Org. Coat.*, 2018, **125**(August), 215–221, DOI: 10.1016/j.porgcoat.2018.09.015.

55 M. Alsaadi, B. Younus, A. Erklig, M. Bulut, O. Bozkurt and B. Sulaiman, Effect of graphene nano-platelets on mechanical and impact characteristics of carbon/Kevlar reinforced epoxy hybrid nanocomposites, *Proc. Inst. Mech. Eng., Part C*, 2021, **235**(23), 7139–7151.

56 D. Gao, Z. Zhao, B. Lyu and J. Ma, Effect of coated and encapsulated polyacrylate/nano-SiO2 composite emulsions on the finishing performances of leather *via* miniemulsion polymerization, *J. Mater. Sci.*, 2020, **55**(23), 10070–10083, DOI: 10.1007/s10853-020-04776-3.

57 Y. Bao, C. Feng, C. Wang, J. Ma and C. Tian, Hygienic, antibacterial, UV-shielding performance of polyacrylate/ZnO composite coatings on a leather matrix, *Colloids Surf., A*, 2017, **518**, 232–240.

58 M. Meyer, S. Dietrich, H. Schulz and A. Mondschein, Leather , and Trendy Alternatives, *Coatings*, 2021, **11**, 226.

59 P. K. Panda, P. Dash, J. M. Yang and Y. H. Chang, Development of chitosan, graphene oxide, and cerium oxide composite blended films: structural, physical, and functional properties, *Cellulose*, 2022, **29**(4), 2399–2411, DOI: 10.1007/s10570-021-04348-x.